Asian Journal of Chemistry; Vol. 35, No. 7 (2023), 1598-1602

ASIAN JOURNAL OF CHEMISTRY

https://doi.org/10.14233/ajchem.2023.27466

Luminescence Properties of Yb^{3+}/Ho^{3+} doped $GdPO_4$ Nanocomposites Prepared by Hydrothermal Method using PEG(6000)

GIRIJA VENKATESWARA KONERU[1], SIRISHA BANDI[1,2] and VENKATA NAGENDRA KUMAR PUTTA[1,*]

[1]Department of Chemistry, GITAM Deemed to be University, Rudraram, Hyderabad-502329, India
[2]B.V. Raju Institute of Technology, Narsapur-502313, India

*Corresponding author: E-mail: vputta@gitam.edu

Received: 26 December 2022; *Accepted*: 6 May 2023; *Published online*: 6 July 2023; AJC-21280

By using hydrothermal synthesis, a novel Yb^{3+}/Ho^{3+} co-doped $GdPO_4$ nanophosphors were prepared which shows both upconversion (UC) and downconversion (DC) with excellent luminescence properties. DC peaks were observed at ~460, ~550, ~650 and ~750 nm. By excitation at 300 nm, a very faint P-O charge transfer (CT) band of Ho^{3+} ions, as well as a tiny non-radiative resonance energy transfer was observed. It is discovered that $GdPO_4$: Yb^{3+}/Ho^{3+}, an upconversion (UC) nanophosphor, enables the production and enhancement of luminescence on a vast scale. On strong 980 nm laser illumination, the upconversion emission spectra show a conspicuous expectant peak of the Ho^{3+} ion at ~550 and ~650 nm. This process yields high-quality nanocrystalline materials with sizes between a few to tens of nm range. Considering the results of the study at 300 nm excitation, $GdPO_4$: Yb^{3+}/Ho^{3+} produced a high quantum yield value. The findings are useful for creating efficient phosphors and it proves applications of nanophosphor materials covered by this method are numerous.

Keywords: Lanthanides(III), Hydrothermal method, Upconversion, Downconversion nanophosphors, Photoluminescence.

INTRODUCTION

When activated by a near-infrared (NIR) laser, the majority of lanthanide ion-doped materials generate the visible radiation [1]. Due to their simple synthesis, lanthanides based materials are receiving more and more attention. Different lanthanides-doped nanomaterials have been developed and employed in a variety of applications, including solar cells, temperature sensors, spectrum converters and biological areas [2]. A poor protocol has been in place up until now for the mass fabrication of up & downconversion nanomaterials. Fascinatingly, lanthanides orthophosphates [3] are frequently referred to as important hosts for the adsorption of nuclear waste due to their strong thermal (up to 2100 ºC) and chemical stability, plausible optical properties and poor solubility. In recent studies, polyol synthesis is a versatile wet-chemistry approach to the design and manufacture of functional inorganic nanoparticles [4,5].

In accumulation, $GdPO_4$ nanoparticles are utilized as a host for (DC)/(UC) luminescence because of this method's ability to modify the size and shape, which can improve the luminous property upon continuous wave (CW) laser stimulation. This will be caused by the acceptable transition, which involves the charge transfer (CT) process of O^{2-} toward Gd^{3+}, which has an intense absorption at 300 nm and absorbs light from 240 to 280 nm. Depending on UV light, one can observe the emission spectrum exhibiting sharpened peaks of the Ho^{3+} ion at ~460, ~550, ~650 and ~750 nm as well as the same peak when excitation is at 300 nm, demonstrating the down-conversion. In this case, Yb^{3+} functions as a sensitizer [6] to increase the strength of Ho^{3+} ion emission in the spectrum, since Ho^{3+} emits intensely when stimulated by near-IR light at about 980 nm. Appearances of the room-temperature emission spectrum about $GdPO_4$ upconversion. The sample was stimulated using a 980 nm laser.

In this study, $GdPO_4$:Ho^{3+}/Yb^{3+} nanophosphor *via* hydrothermal process is developed. Its extraordiniary behaviour has been investigated using excitations at 980 nm (due to Yb^{3+} absorption), 300 nm (due to indirect P-O weak charge transfer band) (CTB) and 460 nm (because of Ho^{3+} absorption) and then discuss about the upconversion, downconversion and energy transfer efficiencies [6]. The sensing characteristics of such particles will increase their effectiveness in optics, display cyber security and microbial systems.

EXPERIMENTAL

As reactants, highly purified analytical grade reagents of Sigma-Aldrich make were utilized. Gadolinium(III) acetate hydrated [$Gd(OAc)_3{\cdot}xH_2O$], ammonium dihydrogen phosphate [$(NH_4)_2HPO_4$], holmium(III) acetate hydrated [$(Ho(OAc)_3){\cdot}xH_2O$], ytterbium(III) acetate hydrated [$Yb(OAc)_3{\cdot}xH_2O$], PEG(6000), HCl, NaOH and deionized water were used as precursors.

Synthesis of $GdPO_4$:Ho^{3+}/Yb^{3+} nanoparticles: The hydrothermal method was employed to prepare the sample. In brief, 730.76 mg of [$Gd(OAc)_3{\cdot}xH_2O$], 8.7 mg of $Ho(OOCCH_3)_3{\cdot}xH_2O$ and 178.48 mg of $Yb(OOCCH_3)_3Yb{\cdot}xH_2O$ were added to 5 mL of conc. HCl and heated until dissolved. To remove excess HCl, alternately added 10 mL of deionized water followed by heating at 80 ºC. The evaporation process was repeated at least five times. In a 100 mL round bottom flask, transferred the evaporated metal ion solution, added 20 mL polyethylene glycol (6000) (PEG) to the mixture, reflux at 75 ºC for at least 10 min, then add $(NH_4)_2HPO_4$ solution dropwise. A yellowish tinge was detected upon the addition of $(NH_4)_2HPO_4$ solution to the round bottom flask. However, the following compounds were transferred to an autoclave and heated in an oven below 120 ºC and below 300 ºC for 4 h and then allowed to cool the compound. We can observe that sample, pale yellow was changed to white colour. A white precipitate eventually developed as a result and allowed to settle to ambient temperature. After the dried powder was centrifuged with demineralized water at 5000 rpm for 5 min, it was washed twice with 10 mL of acetone, dried under an infrared lamp and collected. Calcinated the prepared samples at 900 ºC for 4 h. Similarly, fixed amounts of Yb^{3+} (10 at.%) and Ho^{3+} (3, 5 and 7 at.%) doped $GdPO_4$ nano-particles were generated.

Characterization: Equipment utilizing synchrotrons angle dispersive X-ray diffraction, the sample's average crystal size was investigated (Source: India). Using a scanning electron microscope, microstructural analyses and measurements of the particle size and the surface morphology were obtained. (SEM: quanta) analysis of the vibrational structure of the produced materials was done using 200FTIR spectroscopy, a monochromator (ihr3211, Horiba Jobinn Yvonne) outfitted with a photomultiplier tube that allowed researchers to observe UC emission. To excite the samples, 980 nm light from a diode laser was used. The UC studies deal with the photoluminescence excitation (PLE). Utilizing the excitation WL (wavelength) of an Nd:YAG laser strong ultraviolet excitation at 280-300 nm, the DC emission ranges of $GdPO_4$: Ho^{3+}/Yb^{3+} were studied.

RESULTS AND DISCUSSION

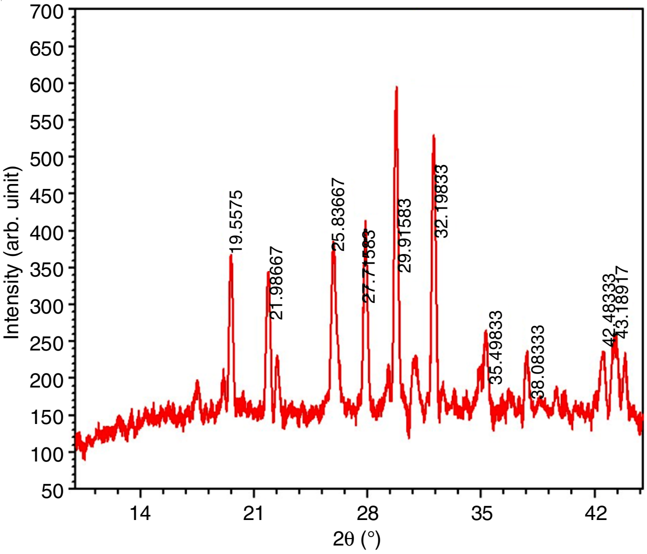

Fig. 1. XRD pattern of $GdPO_4$:Ho^{3+}/Yb^{3+}sample

XRD studies: The XRD patterns of nanophosphor material $GdPO_4$: 1 at. % Ho^{3+} and 20 at. % Yb^{3+} co-doped $GdPO_4$ (also known as $GdPO_4$: Ho^{3+}/Yb^{3+}) and its annealed at 900 ºC are shown in Fig. 1. A strong and sharp peaks that are continuous with the normal monoclinic phase can be seen in the diffraction patterns. The absence of an impurity peak suggests that the dopants are uniformly distributed over the host lattice. Two of the strongest peaks in the XRD diffraction patterns are in a plane that is nearly perpendicular to the plane of the tetragonal structure of pure $GdPO_4$. Based on CN 8, Yb^{3+} and Ho^{3+} ions were substituted at Gd^{3+} positions of the $GdPO_4$ lattice since their ionic radii are similar. In nanophosphor, eight O^{2-} ions are surrounded the Gd^{3+} ion resulting in the formation of pentagonal interpenetrating tetrahedral polyhedron (PITP) geometry with the monoclinic structure of $GdPO_4$.

SEM study: Fig. 2 shows a SEM image of $GdPO_4$:Ho^{3+}/Yb^{3+} nanophosphor material annealed at 900 ºC. The image clearly displays the irregular forms of nanoparticles (a significant proportion of sponge-shaped particles and a small number of (cones, cuboids and spherical shapes). A 50 nm is the typical size obtained from spherical particles.

FTIR: The vibrational structure of the newly prepared $GdPO_4$: Ho^{3+}/Yb^{3+} nanophosphor material was investigated by FTIR spectroscopy (Bomemn MB 104 spectrophotometer) with a resolution of 1 cm^{-1} and is shown in Fig. 3.

Photoluminescence study of $GdPO_4$:Ho^{3+},Yb^{3+}

Upconversion study: Upconversion luminescence is an optical phenomenon that releases high-energy photons while absorbing low-energy photons (multiphoton) and is caused by anti-Stokes luminescence (multiphoton) [7]. Ho^{3+} can release either green or red emission based on the relative concentrations of the host and co-dopant [8]. The upconversion emission spectra for $GdPO_4$: Ho^{3+}/Yb^{3+} (1% Ho^{3+} and 20% Yb^{3+}) at differing laser powers beyond 980 nm of excitation are shown in Fig. 4. The electronic transitions of the Ho^{3+} ion at $^5F_4$, $^5S_2{\rightarrow}{}^5I_8$, $^5F_5{\rightarrow}{}^5I_8$ and 650 nm result in the green emission bands at 550 nm and red emission based on the relative concentrations of the host and co-dopant bands at 650 nm (R = red) in the UC spectra [9,10]. With a higher absorption fraction than Ho^{3+} at 980 nm excitation, Yb^{3+} ions are acting as sensitizers. The excitation spectrum of $GdPO_4$ reveals the P-O charge transfer band (CTB) with a peak at 460 nm, Ho^{3+} emission = 550 nm and emission spectra at the excitation of 300 and 460 nm show the P-O and Ho^{3+} peaks.

Down conversion study: This process involves releasing lower-energy radiation light (emission) after absorbing higher-

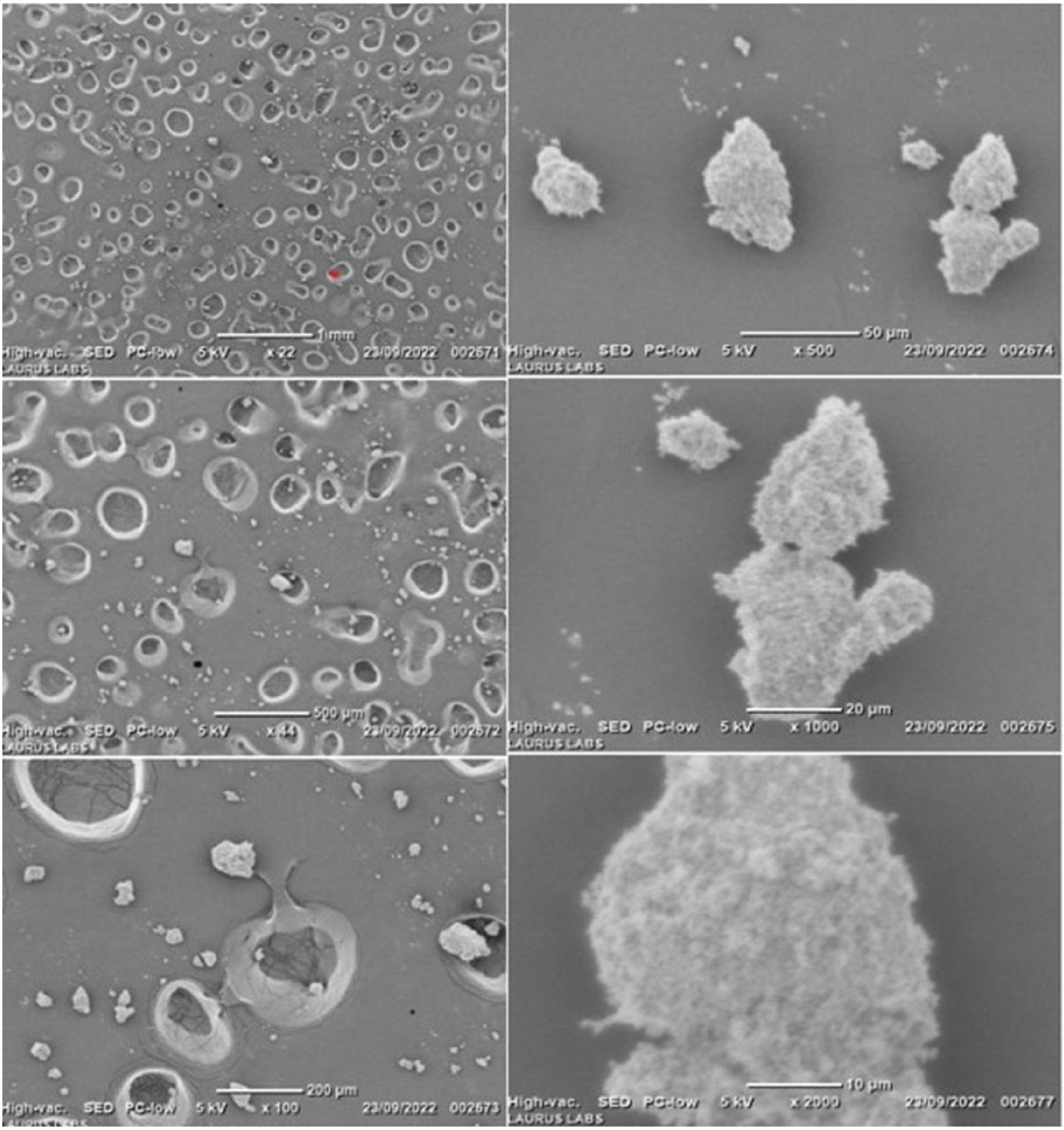

Fig. 2. SEM images of $GdPO_4$:Ho^{3+}/Yb^{3+}

energy light (excitation) [11,12], which results in the occurance of Stokes shift [13]. Fig. 5 depicts the DC emission spectrum of $GdPO_4$:Ho^{3+}/Yb^{3+} (1 at.% Ho) beyond UV excitation at 300 nm [14,15]. The Ho^{3+} ion's $^5F_4$ and $^5S_2 \rightarrow ^5I_8$ and $^5F_5 \rightarrow ^5I_8$ ET'S exhibited the emission bands green (at 550 nm), red (at 650 nm) and NIR (at 750 nm) , respectively. At ~260, ~290, ~300 and ~460 nm, four excitation wavelengths are used to monitor the emission spectra. For each excitation, the Ho^{3+} emission peaks are displayed. When Ho^{3+} is stimulated directly at ~460 nm ($^5I_8 \rightarrow ^5G_6$) instead of indirectly at 300 nm, its emission intensity is weaker. This arises from Ho^{3+} *f-f* transitions, which is due to its low absorption cross-section [16]. When excitation occurs at 300 nm, the broad emission band ~460nm and PO_4^{3-} peaks and peaks of Ho^{3+} are observed. For each excitation, the Ho^{3+} emission peaks are displayed. When Ho^{3+} is directly excited at ~460 nm ($^5I_8 \rightarrow ^5G_6$) as opposed to indirectly excited at ~300 nm, its emission intensity is weaker. This is because the transitions involving Ho^{3+} have a small cross-section for absorption. Peaks of Ho^{3+} and the large emission band associated with PO_4^{3-} at 460 nm are observed for excitation at 300 nm.

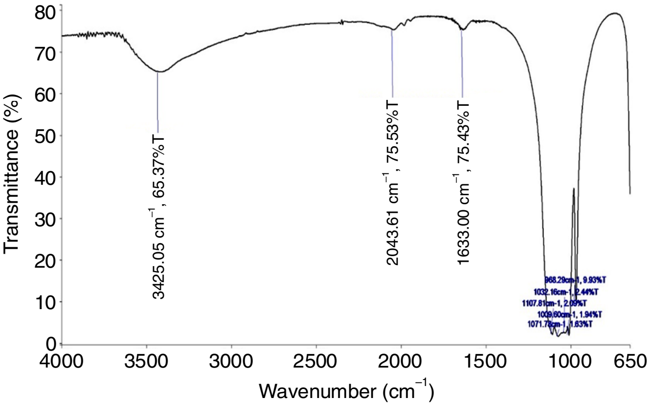

Fig. 3. FTIR of GdPO$_4$:Ho^{3+}/Yb^{3+}

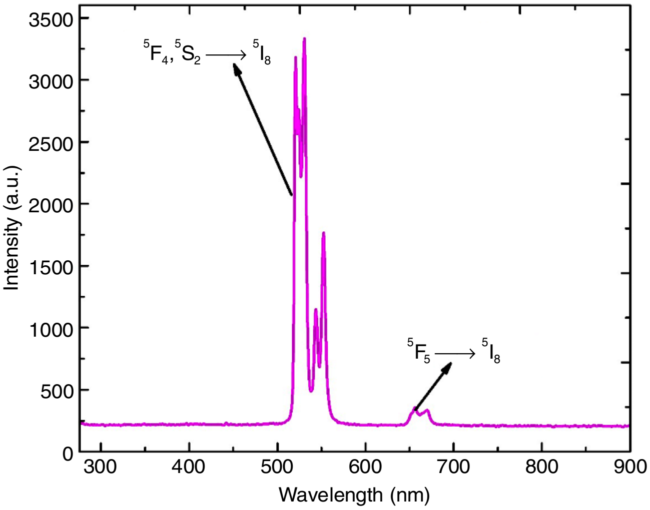

Fig. 4. Emission spectra of GdPO$_4$: Ho^{3+}/Yb^{3+}(1 at.%Ho) excited at 980 nm

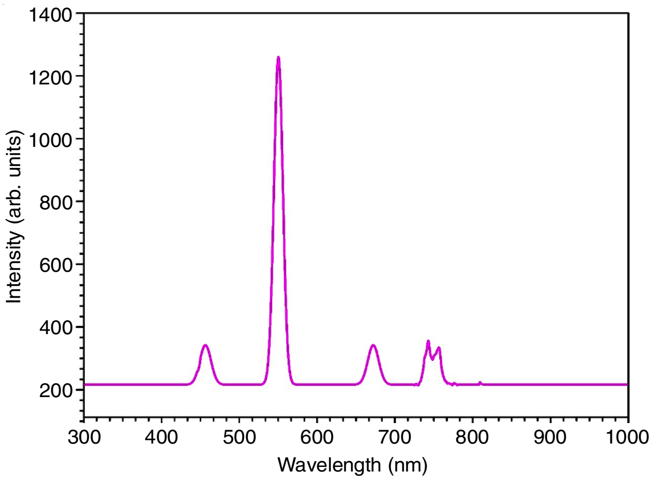

Fig. 5. Excitation spectrum of GdPO$_4$:Ho^{3+}/Yb^{3+}(1 at.% Ho) excited at 300 and 460 nm

The P-O charge transfer band allowed transition results in a significant absorption cross-section at 300 nm. As a significant proportion of exciting photons from P-O are de-excited and the exciting energy is transferred from P-O to Ho^{3+}, the radiative rate of Ho^{3+} rises. This is the hypothetical resonance transition of electrons from PO_4^{3-} to Ho^{3+}. Fig. 5 displays the monitoring of GdPO$_4$:Ho^{3+}/Yb^{3+} emission at 550 nm. A broad peak, having the highest point at 300 nm is observed from 260 to 360 nm, which relates to the permitted P-O charge transfer band transition. Sharp peaks with low intensities were found at 460 nm due to Ho^{3+} (~550-580 nm). To demonstrate the concentration-dependent luminescence (20 at%), the GdPO$_4$ host is doped with or different concentrations of Ho^{3+} at the prescribed concentration of Yb^{3+} [17]. The GdPO$_4$:Ho^{3+}, Yb^{3+} (x at.% = 1, y at.% = 20) shows the emission peaks of Ho^{3+} when stimulated at 300 nm and 460 nm. The light intensity reduces when the Ho^{3+} ion concentration upswings by 1%. (Fig. 5). The key element is the concentration quenching effect [18,19].

Conclusion

In this work, GdPO$_4$:0.01Ho^{3+}/0.2Yb^{3+} nanophosphor material was effectively synthesized using a hydrothermal mediated method. The XRD results showed that the sample had a improved monoclinic structural phase with space group 141/amd after being annealed for 4 h at 900 ºC. Strong up convertion green and red colour bands were produced by GdPO$_4$:0.01Ho^{3+}/0.2Yb^{3+} at 550 nm ($^5F_4$, $^5S_2 \rightarrow {}^5I_8$) and 650 nm ($^5F_5 \rightarrow {}^5I_8$) of Ho^{3+} under 980 nm illumination. At 300 nm excitation, a wide emission peak at ~460 nm, ~550 nm ($^5F_4$, $^5S_2 \rightarrow {}^5I_8$), ~650 nm ($^5F_5 \rightarrow {}^5I_8$), ~750 nm ($^5F_4$, $^5S_2 \rightarrow {}^5I_7$) and Ho^{3+} characteristic peaks were found. The broad emission band was mostly due to the charge transfer band from ligand to the metal due to lower conversion rates (P-O). According to the down conversion study, the generation of green and red lines was due to the two-photon absorption.

CONFLICT OF INTEREST

The authors declare that there is no conflict of interests regarding the publication of this article.

REFERENCES

1. C. Cao, Q. Liu, M. Shi, W. Feng and F. Li, *Inorg. Chem.*, **58**, 9351 (2019); https://doi.org/10.1021/acs.inorgchem.9b01071
2. B. Li, F. Tian, X. Cui, B. Xiang, H. Zhao, H. Zhang, D. Wang, J. Li, X. Wang, X. Fang, M. Qiu and D. Wang, *Nanomaterials*, **12**, 1773 (2022); https://doi.org/10.3390/nano12101773
3. R.S. Perala, R. Joshi, B.P. Singh, V.N.K. Putta, R. Acharya and R.S. Ningthoujam, *ACS Omega*, **6**, 19471 (2021); https://doi.org/10.1021/acsomega.1c01572
4. S. Ammar and F. Fiévet, *Nanomaterials*, **10**, 1217 (2020); https://doi.org/10.3390/nano10061217
5. F. Fiévet, S. Ammar-Merah, R. Brayner, F. Chau, M. Giraud, F. Mammeri, J. Peron, J.-Y. Piquemal, L. Sicard and G. Viau, *Chem. Soc. Rev.*, **47**, 5187 (2018); https://doi.org/10.1039/C7CS00777A
6. R.S. Perala, B.P. Singh, V.N.K. Putta, R. Acharya and R.S. Ningthoujam, *ACS Omega*, **6**, 19517 (2021); https://doi.org/10.1021/acsomega.1c01813
7. Q. Liu, W. Feng, T. Yang, T. Yi and F. Li, *Nat. Protoc.*, **8**, 2033 (2013); https://doi.org/10.1038/nprot.2013.114
8. N. Yaiphaba, R.S. Ningthoujam, N.R. Singh and R.K. Vatsa, *Eur. J. Inorg. Chem.*, **2010**, 2682 (2010); https://doi.org/10.1002/ejic.200900968
9. V. Kumar, P. Rani, D. Singh and S. Chawla, *RSC Adv.*, **4**, 36101 (2014); https://doi.org/10.1039/C4RA04795H
10. V. Kumar and G. Wang, *J. Lumin.*, **199**, 188 (2018); https://doi.org/10.1016/j.jlumin.2018.03.037
11. A. Dwivedi, E. Rai, D. Kumar and S.B. Rai, *ACS Omega*, **4**, 6903 (2019); https://doi.org/10.1021/acsomega.8b03606

12. A. Mahata, K.S. Rawat, I. Choudhuri and B. Pathak, *Sci. Rep.*, **6**, 25590 (2016); https://doi.org/10.1038/srep25590
13. A.K. Parchur, A.A. Ansari, B.P. Singh, T.N. Hasan, N.A. Syed, S.B. Rai and R.S. Ningthoujam, *Integr. Biol.*, **6**, 53 (2014); https://doi.org/10.1039/C3IB40148K
14. F. Hu, X. Wei, Y. Qin, S. Jiang, X. Li, S. Zhou, Y. Chen, C.-K. Duan and M. Yin, *J. Alloys Compd.*, **674**, 162 (2016); https://doi.org/10.1016/j.jallcom.2016.03.040
15. W. Ren, G. Tian, L. Zhou, W. Yin, L. Yan, S. Jin, Y. Zu, S. Li, Z. Gu and Y. Zhao, *Nanoscale*, **4**, 3754 (2012); https://doi.org/10.1039/c2nr30683b
16. Z. Wang, J. Feng, M. Pang, S. Pan and H. Zhang, *Dalton Trans.*, **42**, 12101 (2013); https://doi.org/10.1039/c3dt51010g
17. Yu. Gao, Y. Qiu, X. Wang, Y. Bi, G. Zhao, F. Ding, Y. Sun and Z. Xu, *RSC Adv.*, **8**, 21857 (2018); https://doi.org/10.1039/C8RA04198A
18. G.A. Kumar, N.R. Balli, M. Kailasnath, L.C. Mimun, C. Dannangoda, K.S. Martirosyan, C. Santhosh and D.K. Sardar, *J. Alloys Compd.*, **672**, 668 (2016); https://doi.org/10.1016/j.jallcom.2016.02.165
19. C. Cao, H.K. Yang, B.K. Moon, B.C. Choi and J.H. Jeong, *J. Electrochem. Soc.*, **158**, J6 (2011); https://doi.org/10.1149/1.3517458